Available online at www.sciencedirect.com

ScienceDirect

Transportation Research Procedia 6 (2015) 172 – 188

Transportation Research Procedia

www.elsevier.com/locate/procedia

4th International Symposium of Transport Simulation-ISTS'14, 1-4 June 2014, Corsica, France

Dynamic estimation of headway distance in vehicle platoon system under unexpected car-following situations

Hironori Suzuki [a,*], Takashi Nakatsuji [b]

[a] *School of Mechanical System Engineering, Nippon Institute of Technology, 4-1 Gakuendai, Miyashiro, Saitama 3458501, Japan*

[b] *Faculty of Engineering, Hokkaido University, North 13, West 8, Sappporo, Hokkaido 0608628, Japan*

Abstract

The headway distance between vehicles in a platoon is difficult to measure unless the vehicles are equipped with costly equipment such as laser or radar sensors, or an image processing system. This paper proposes an alternate approach to estimating headway distance indirectly from measurable variables such as the acceleration rate and velocity of selected vehicles in the platoon. Assuming a six-vehicle platoon, a particle filter (PF) and an unscented Kalman filter (UKF) are applied in order to estimate the headway of each vehicle based on the measurement variables of three (or all) vehicles in the platoon. The state-space models of the PF and the UKF are given by the conservation equation of headway and the conventional car-following model. To evaluate the PF and UKF performance, two scenarios were prepared: one assumed that prior knowledge of a model parameter differed from what was actually observed as posterior information, the other was a situation where a platoon vehicle slowed down unexpectedly during the car-following process. In both situations, the state-space model itself was unable to describe the dynamics of headway distance precisely, and the PF and the UKF were applied to minimize the headway distance errors caused by the incorrect model parameter and the unexpected vehicle slowdown. Numerical analysis demonstrated that both the PF and UKF were successful in estimating the headway distance, even when the car-following model did not express the true car-following phenomena. We also determined that, if all vehicles are equipped as probe cars, and thus capable of measuring the acceleration rate and velocity, the PF is superior to UKF when estimating the headway distance precisely. However, UKF is more stable than the PF when measurements are not taken from all vehicles, especially when a vehicle in the platoon unexpectedly slows downs during the car-following process.

Selection and/or peer-review under responsibility of the Organizing Committee of ISTS'14

* Corresponding author. Tel.: +81-480-33-7734; fax: +81-480-33-7663.
E-mail address: viola@nit.ac.jp

Selection and/or peer-review under responsibility of the Organizing Committee of ISTS'14
doi:10.1016/j.trpro.2015.03.014

Keywords: dynamic estimation; vehicle platoon, particle filter; unscented Kalman filter

1. Introduction

The headway distance of longitudinal car-following vehicles is the most important parameter when evaluating the risk of front-to-rear-end collisions [Takada et al.(2012); Marumo et al.(2013)]. The automatic collision avoidance systems that have been developed by many vehicle manufactures to date "directly" measure the headway distance between vehicles using on-board distance measurement sensors. However, such sensors are too expensive to be installed on all of the vehicles in a platoon. Therefore, instead of the direct measurements, estimating or calculating the headway distance "indirectly" from measurable variables is a preferable technique.

In previous studies, the authors have applied particle filters (PFs), unscented Kalman filters (UKFs), and extended Kalman filters (EKFs) to the problem of dynamic headway distance estimations in a platoon system [Suzuki and Nakatuji (2013); Suzuki (2013)]. The PF and UKF are especially well known as powerful tools, and have been widely applied to various dynamic estimation problems including traffic state estimations [Pueboobpaphan et al., 2007], estimation of an origin-destination matrix [Pueboobpaphan and Nakatsuji (2011)], estimating visual shape and motion [Blake et al., 2001], mobile robot control [Fox et al., 2001], target tracking [McGinnity and Irwin (2001)], among others. Our previous study also showed that they are superior to other conventional estimation methods, including EKF, in estimating the headway distance of each vehicle in a platoon.

In this study, the state-space model of feedback estimators is defined by the conservation equation of headway and the conventional car-following model. The conservation equation is used as the state equation of the state-space model, whereas the car-following model is used for the measurement equation.

As explained above, the PF and the UKF perform extremely well in estimating the headway distance of platooned vehicles if the measurement equation calculates the acceleration rate precisely [Suzuki and Nakatsuji (2013)]. However, in an actual platoon situation, the state-space model is not always able to describe actual car-following behavior. In other words, the real acceleration and deceleration behavior of human drivers are not always equal to the calculation outputs provided by the theoretical car-following model. This is especially true when a vehicle in the platoon slows down unexpectedly. In such situations, the headway distance behavior is significantly different from the results computed by the theoretical model. Therefore, even in situations where the model does not precisely describe actual car-following behavior, headway estimations should be as accurate as possible in order to provide sufficient levels of precision.

In the present research, we prepared different car-following model parameter sets for use when generating observation data, beginning with the assumption that the prior information on model parameters would be different from actual posterior observations. Additionally, it is assumed that a vehicle in a platoon would slow down unexpectedly during the car-following process. We then evaluated the performance of the PF and the UKF by determining how capable they were of minimizing errors caused by the model parameter deviation and the unexpected vehicle slowdown.

2. Theoretical background

2.1. State-space model

The following state and measurement equations are defined as the state-space model:

$$\mathbf{x}_k = \mathbf{f}\left(\mathbf{x}_{k-1}, \mathbf{u}_{k-1}\right) + \mathbf{v}_{k-1}, \tag{1}$$

$$\mathbf{y}_k = \mathbf{g}\left(\mathbf{x}_k\right) + \mathbf{w}_k, \tag{2}$$

where, $\mathbf{x}_k$ and $\mathbf{y}_k$ are the state and measurement variables at time k, $\mathbf{v}_k$ and $\mathbf{w}_k$ are the corresponding system and measurement errors, $\mathbf{f}$ and $\mathbf{g}$ are the possible non-linear functions, and $\mathbf{u}_k$ is the control variable. In this research, $\mathbf{x}_k$ is denoted as the headway distance and velocity of each vehicle and $\mathbf{y}_k$ shows the acceleration rate and velocity measured at preselected vehicles in a platoon.

Let $\mathbf{y}_{1:k}$ and $\mathbf{x}_{1:k}$ denote as a set of all available measurement and state variables up to time k:

$$\mathbf{y}_{1:k} \equiv \{\mathbf{y}_1, \mathbf{y}_2, \ldots, \mathbf{y}_k\} \text{ and } \mathbf{x}_{1:k} \equiv \{\mathbf{x}_1, \mathbf{x}_2, \ldots, \mathbf{x}_k\} . \tag{3}$$

The estimation problem is calculating the posterior probability $p(\mathbf{x}_k|\mathbf{y}_{1,k})$ when giving a set of all measurements $\mathbf{y}_{1:k}$. If $\mathbf{y}_k$ is available, the posterior is updated through the Bayes' rule:

$$p(\mathbf{x}_k|\mathbf{y}_{1,k}) = \frac{p(\mathbf{x}_k|\mathbf{y}_{1,k-1}) \cdot p(\mathbf{y}_k|\mathbf{x}_k)}{p(\mathbf{y}_k|\mathbf{y}_{1,k-1})} \tag{4}$$

Here, $p(\mathbf{y}_k|\mathbf{x}_k)$ is a likelihood function which describes the likelihood of $\mathbf{y}_k$ given the $\mathbf{x}_k$. $p(\mathbf{x}_k|\mathbf{y}_{1,k-1})$ is a prior probability of $\mathbf{x}_k$ given by:

$$p(\mathbf{x}_k|\mathbf{y}_{1,k-1}) = \int p(\mathbf{x}_k|\mathbf{x}_{k-1}) \cdot p(\mathbf{x}_{k-1}|\mathbf{y}_{1,k-1}) d\mathbf{x}_{k-1} \tag{5}$$

Additionally, $p(\mathbf{y}_k|\mathbf{y}_{1,k})$ is defined as

$$p(\mathbf{y}_k|\mathbf{y}_{1,k-1}) = \int p(\mathbf{y}_k|\mathbf{x}_k) \cdot p(\mathbf{x}_k|\mathbf{y}_{1,k-1}) d\mathbf{x}_k \tag{6}$$

$p(\mathbf{x}_k|\mathbf{x}_{k-1})$ in (5) and $p(\mathbf{y}_k|\mathbf{x}_k)$ in (6) can be given by the state and measurement equations (1) and (2). In a conventional EKF and UKF, there is a strong requirement that the posterior and prior probability density functions (PDFs) $p(\mathbf{x}_k|\mathbf{y}_{1,k})$ and $p(\mathbf{x}_k|\mathbf{y}_{1,k-1})$ be Gaussian, whereas the PF does not impose any assumptions or analytical functions on the PDFs.

2.2. Particle filter (PF)

2.2.1. Theory

The primary purpose of using a PF is to represent the required posterior PDF by a set of random samples with associated weights, and to compute the estimates based on these samples and weights [Doucet & Johansen, 2011; Arulampalam *et al.*, 2002; Ikoma, 2012].

Let $\left\{\left(x_{1:k-1}^{(i)}, w_{1:k-1}^{(i)}\right)\right\}_{i=1}^{M}$ denote a set of particles and its associated weights. It is assumed that $\left\{\left(x_{1:k-1}^{(i)}, w_{1:k-1}^{(i)}\right)\right\}_{i=1}^{M}$ is given by the posterior PDF at time $k-1$. When providing the measurement $\mathbf{y}_k$ at time step k, the PF computes and updates the particles and weights from $\left\{\left(x_{1:k-1}^{(i)}, w_{1:k-1}^{(i)}\right)\right\}_{i=1}^{M}$ into $\left\{\left(x_{1:k}^{(i)}, w_{1:k}^{(i)}\right)\right\}_{i=1}^{M}$.

Weight is updated through a process called sequential importance sampling (SIS). SIS generates particles based on the proposal distribution $q(\mathbf{x})$, which differs from the objective distribution $f(\mathbf{x})$, and then gives each particle its appropriate weight in order to position the particles close to the objective PDF.

The weight update process is given by

$$\tilde{w}_k^{(i)} = w_k^{(i)} \frac{f\left(\tilde{x}_k^{(i)} \middle| x_{k-1}^{(i)}\right) g\left(y_k \middle| x_k^{(i)}\right)}{q\left(\tilde{x}_k^{(i)} \middle| x_{1:k-1}^{(i)}, y_{1,k}\right)} \left(i = 1, 2, ..., M\right) \tag{7}$$

The PF is a feedback estimator that theoretically places the random particles in the probability field in order to yield an accurate posterior PDF based on Bayes' theory. It is guaranteed that the estimates obtained via the filtering process are suboptimal.

2.2.2. Estimation algorithm by PF

Since the measurement equation (2) does not always express real observation data, the proposal distribution $q(\mathbf{x})$ should be introduced in order to generate samples for every time step in order to accommodate the area where the system model (1) itself is unable to cover the one-step prediction. The PF estimation algorithm is as follows:

1. Generate particles at time step k from the system model $\mathbf{f}(\cdot)$ and the additive zero-mean Gaussian system noise. As an alternate approach, the particles may be generated by the proposal distribution $q(\mathbf{x})$. The use of proposal $q(\mathbf{x})$ enables particles to be generated in the area that cannot be covered by one-step prediction:

$$\tilde{\mathbf{x}}_k^{(i)} \sim \mathbf{f}\left(\hat{\mathbf{x}}_{k-1}^{(i)}, \mathbf{u}_{k-1}\right) + \mathbf{v}_{k-1}. \tag{8}$$

2. Compute the one-step prediction of measurement variables $\tilde{\mathbf{y}}_k^{(i)}$ from the measurement model $\mathbf{g}(\cdot)$ and the zero-mean additive Gaussian measurement noise:

$$\tilde{\mathbf{y}}_k^{(i)} \sim \mathbf{g}\left(\tilde{\mathbf{x}}_k^{(i)}\right) + \mathbf{w}_k. \tag{9}$$

3. Calculate the weight of each particle by (10). In this research, for example, the evaluation distribution is given by the Gaussian whose standard deviation is $\mathbf{w}_k$. As defined in (10), larger weight is given to the particles for which the prediction $\tilde{\mathbf{y}}_k^{(i)}$ is closer to the actual measurement $\mathbf{y}_k$.

$$\tilde{w}_k^{(i)} = N\left(\mathbf{y}_k - \tilde{\mathbf{y}}_k^{(i)}, \mathbf{w}_k\right) \tag{10}$$

4. Normalize the weight $\tilde{w}_k^{(i)}$ between 0 and 1.
5. Compute the effective sample size (*ESS*) by (11).

$$ESS = 1 \Big/ \sum_{i=1}^{M} \left(\tilde{w}_k^{(i)}\right)^2 \tag{11}$$

6. If *ESS* is smaller than the threshold *ESSTH*, the particle $\tilde{\mathbf{x}}_k^{(i)}$ is resampled in proportion to the importance weight $\tilde{w}_k^{(i)}$.

$$\hat{\mathbf{x}}_k^{(i)} \sim \begin{cases} \tilde{\mathbf{x}}_k^{(1)} & with\ prob.\ \tilde{w}_k^{(1)} \\ \tilde{\mathbf{x}}_k^{(2)} & with\ prob.\ \tilde{w}_k^{(2)} \\ \quad\vdots & \\ \tilde{\mathbf{x}}_k^{(M)} & with\ prob.\ \tilde{w}_k^{(M)} \end{cases}, \tag{12}$$

If the particles are resampled, the importance weight is reset to the constant:

$$\hat{w}_k^{(i)} = 1/M\ . \tag{13}$$

Otherwise, the samples and weights remain unchanged:

$$\hat{\mathbf{x}}_k^{(i)} = \tilde{\mathbf{x}}_k^{(i)}, \quad \hat{w}_k^{(i)} = \tilde{w}_k^{(i)}. \tag{14}$$

7. Compute the expectation of state variables as the mean by

$$\hat{\mathbf{x}}_k = \frac{1}{M}\sum_{i=1}^{M} \hat{\mathbf{x}}_k^{(i)} \left(= \sum_{i=1}^{M} \hat{w}_k^{(i)} \hat{\mathbf{x}}_k^{(i)} \right). \tag{15}$$

2.3. Unscented Kalman Filter (UKF)

The UKF is a *derivative-free* Kalman filter that requires no calculation of partial derivatives for the state and measurement equations [Wan and Nelson (2001)]. The conventional EKF provides a first-order approximation to the optimal estimates, whereas the UKF can accurately obtain the posterior mean and covariance to their second-order Taylor expansions using a minimal set of carefully chosen sample points, called sigma points [Wan and Nelson (2001)]. The first step in the application of the UKF is to generate the sigma point $\tilde{\mathbf{\Phi}}_k$ as

$$\boldsymbol{\sigma}_{i,P} = \left(\sqrt{(N+\lambda)\mathbf{P}_k} \right)_i, \tag{16}$$

$$\hat{\Phi}_{0,k-1} = \hat{\mathbf{x}}_0, \quad \hat{\Phi}_{i,k-1} = \hat{\mathbf{x}}_{k-1} + \boldsymbol{\sigma}_{i,P} \left(i = 1,\ldots,N \right), \quad \hat{\Phi}_{i,k-1} = \hat{\mathbf{x}}_{k-1} - \boldsymbol{\sigma}_{i-N,P} \left(i = N+1,\ldots,2N \right), \tag{17}$$

$$\tilde{\mathbf{\Phi}}_k = \mathbf{f}\left(\hat{\mathbf{\Phi}}_{k-1} \right), \tag{18}$$

where $\boldsymbol{\sigma}_i$ is the i -th column vector of the lower triangle matrix when applying the Cholesky decomposition to the error covariance $\mathbf{P}_k$, N is the number of state variables, and λ is the scaling parameter. The mean of the state variables and the error covariance before the observation are then given by

$$\textit{(mean before observation)}\ \ \tilde{\mathbf{x}}_k = \sum_{i=0}^{2N} h_i \tilde{\Phi}_{i,k}, \tag{19}$$

$$\textit{(covariance before observation)}\ \ \mathbf{M}_k^{xx} = \sum_{i=0}^{2N} h_i \left[\tilde{\Phi}_{i,k} - \tilde{\mathbf{x}}_k \right] \left[\tilde{\Phi}_{i,k} - \tilde{\mathbf{x}}_k \right]^T + \mathbf{V}_{k-1}. \tag{20}$$

where $\mathbf{V}_{k-1}$ is the covariance of system error and h_i is the weight defined by

$$h_i = 1/2\left(N+\lambda\right). \tag{21}$$

The same procedure is applied to compute $\tilde{\mathbf{y}}_k$, $\mathbf{M}_k^{yy}$, and $\mathbf{M}_k^{xy}$ by defining the sigma vectors $\tilde{\boldsymbol{\Psi}}_k$, $\tilde{\boldsymbol{\Omega}}_k$, and the covariance of measurement vector $\mathbf{W}_{k-1}$:

$$\boldsymbol{\sigma}_{i,M} = \left(\sqrt{\left(N+\lambda\right)\mathbf{M}_k}\right)_i, \tag{22}$$

$$\tilde{\Omega}_{0,k-1} = \tilde{\mathbf{x}}_0, \quad \tilde{\Omega}_{i,k} = \tilde{\mathbf{x}}_k + \boldsymbol{\sigma}_{i,M}\left(i=1,\ldots,N\right), \quad \tilde{\Omega}_{i,k} = \tilde{\mathbf{x}}_k - \boldsymbol{\sigma}_{i,M}\left(i=N+1,\ldots,2N\right) \tag{23}$$

$$\tilde{\boldsymbol{\Psi}}_k = \mathbf{g}\left(\tilde{\boldsymbol{\Omega}}_k\right), \tag{24}$$

$$\tilde{\mathbf{y}}_k = \sum_{i=0}^{2N} h_i \tilde{\Psi}_k, \tag{25}$$

$$\mathbf{M}_k^{yy} = \sum_{i=0}^{2N} h_i \left[\tilde{\Psi}_{i,k} - \tilde{\mathbf{y}}_k\right]\left[\tilde{\Psi}_{i,k} - \tilde{\mathbf{y}}_k\right]^T + \mathbf{W}_{k-1} \quad , \tag{26}$$

$$\mathbf{M}_k^{xy} = \sum_{i=0}^{2N} h_i \left[\tilde{\Phi}_{i,k} - \tilde{\mathbf{x}}_k\right]\left[\tilde{\Psi}_{i,k} - \tilde{\mathbf{y}}_k\right]^T. \tag{27}$$

The Kalman gain is then computed from the error covariance $\mathbf{M}_k^{yy}$ and $\mathbf{M}_k^{xy}$ by (28). Mean and error covariance $\hat{\mathbf{x}}_k$ and $\mathbf{P}_k$ are finally updated after the observation by using (29) and (30).

$$\mathbf{K}_k = \mathbf{M}_k^{xy}\left(\mathbf{M}_k^{yy}\right)^{-1}, \tag{28}$$

$$\textit{(mean \underline{after} observation)}\ \hat{\mathbf{x}}_k = \tilde{\mathbf{x}}_k + \mathbf{K}_k\left(\mathbf{y}_k - \tilde{\mathbf{y}}_k\right). \tag{29}$$

$$\textit{(covariance \underline{after} observation)}\ \mathbf{P}_k = \mathbf{M}_k^{xx} - \mathbf{K}_k\mathbf{M}_k^{xx}\mathbf{K}_k^T. \tag{30}$$

Equations (29) and (30) show that the mean is shifted to a location close to the true mean and that the error covariance is smaller than that computed before the observation. However, UKF is strongly limited by the fact that the state variables must follow the Gaussian distribution, whereas the PF has no probability distribution function limitations.

3. State-space model for six-vehicle platoon

3.1. Modeling the dynamics of headway distance and velocity

Assuming that six vehicles form a longitudinal platoon system as depicted in Fig. 1, the dynamics of headway and velocity of each platooned vehicle are formulated as the difference equations

$$\ell_k^i = \ell_{k-1}^i + \left[v_{k-1}^{i-1} - v_{k-1}^i\right]\Delta t \tag{31}$$

$$v_k^i = v_{k-1}^i + a_{k-1}^i \Delta t \,. \tag{32}$$

Here, ℓ_k^i, v_k^i, and a_k^i are headway distance, velocity, and acceleration rate of the vehicle i at time k. Δt is a discrete time step.

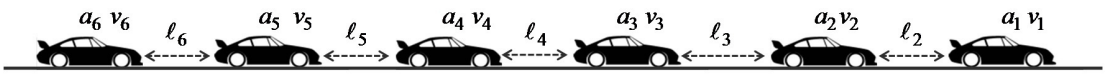

Fig. 1: Six-vehicle platoon

The acceleration rate in (32) is given by a conventional car-following model, which is well known as the Gazis-Herman-Rotery (GHR) model [Rothery (1998)]:

$$a_{k+T}^i = \alpha \frac{\left(v_k^i\right)^n}{\left(\ell_k^i\right)^m}\left[v_k^{i-1} - v_k^i\right] \,. \tag{33}$$

where, α, m, n are the model parameters and T is defined as the vehicle reaction time. For simplicity, the reaction time is assumed to be zero, i.e., $T = 0$, under the assumption that errors due neglecting T will be minimized by the estimator feedback process. Substituting (33) into (32) redefines the velocity as

$$v_k^i = v_{k-1}^i + \alpha \frac{\left(v_{k-1}^i\right)^n}{\left(\ell_{k-1}^i\right)^m}\left[v_{k-1}^{i-1} - v_{k-1}^i\right]\Delta t \,. \tag{34}$$

If velocity is also chosen as a measurement variable, the additional measurement equation is

$$v_k^i = v_k^i \,. \tag{35}$$

Equations (31) and (34) are regarded as the state equations, whereas (33) and (35) can be used as the measurement equation for the state-space model of a vehicle platoon.

4. Numerical analysis

4.1. Preparing evaluation and measurement data sets

Given the velocity of the 1st vehicle of the platoon, the evaluation data on headway distance are computed by executing the system models (31) and (34). It should be noted that the model parameters are set to α=m=n=1. The acceleration rate and velocity are also calculated by the measurement models (33) and (35) to be used as the real observation data.

When creating the evaluation and measurement data, the covariance of system noise is set to 0.1 for headway and 0.05 for velocity, whereas the measurement noise covariance are fixed at 0.005 for acceleration rate and 0.01 for velocity.

4.2. Selection of probe car(s)

In this study, a "probe car" is defined as a vehicle that is equipped with the sensors necessary to measure the vehicle's acceleration rate and velocity. The estimation problem is determining how precisely the PF and the UKF estimate the headway distance of each vehicle in the platoon by measuring the acceleration rate and velocity at the probe cars. This research assumes the following two cases:

- The 2nd, 4th, and 6th vehicles are equipped as probe cars.
- All five following vehicles are equipped as probe cars.

It is assumed that the velocity of the 1st vehicle is externally given to the system as the input. The state and measurement variables for each scenario are then defined as

$$\mathbf{x}_k = \left[\ell_2, v_2, ..., \ell_6, v_6\right]^T_{(k)}, \mathbf{y}_k = \left[a_2, v_2, a_4, v_4, a_6, v_6\right]^T_{(k)}, \tag{36}$$

$$\mathbf{x}_k = \left[\ell_2, v_2, ..., \ell_6, v_6\right]^T_{(k)}, \mathbf{y}_k = \left[a_2, v_2, ..., a_6, v_6\right]^T_{(k)}. \tag{37}$$

The car-following process is not a steady-state flow, but is, instead, an unstable state that requires continuous acceleration and deceleration actions in short time periods. The speed profile of the 1st vehicle is given in Fig. 2.

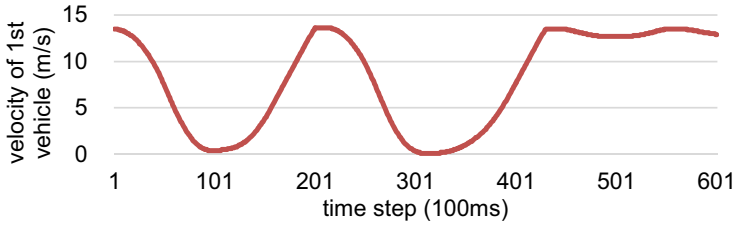

Fig. 2: Velocity of 1st vehicle

4.3. Two cases that deviate the headway distance from the true observation

Two cases were prepared to express situations where the car-following model is incapable of calculating the headway distance. The first is the case where the parameter set of the car-following model is different from what is actually observed, and the other is a situation where a vehicle unexpectedly slows down during the car-following process. In both cases, the actually observed headway distance is different from the output of the GHR car-following model. This study hypothesizes that the PF and UKF feedback processes will minimize the deviation.

4.3.1. Incorrect model parameters

In the real world, it is self-evident that the model parameter setting α=m=n=1 can never be guaranteed. Accordingly, this research assumes other model parameter values α=0.8, m=1.2, n=1.1 as the prior knowledge when estimating the headway distance.

Different model parameters yield different model output, as depicted in Fig. 3, where it can be clearly seen that the incorrect model parameter set (α=0.8, m=1.2, n=1.1) results in a headway distance deviation from the actual one given by correct parameter set, α=m=n=1.

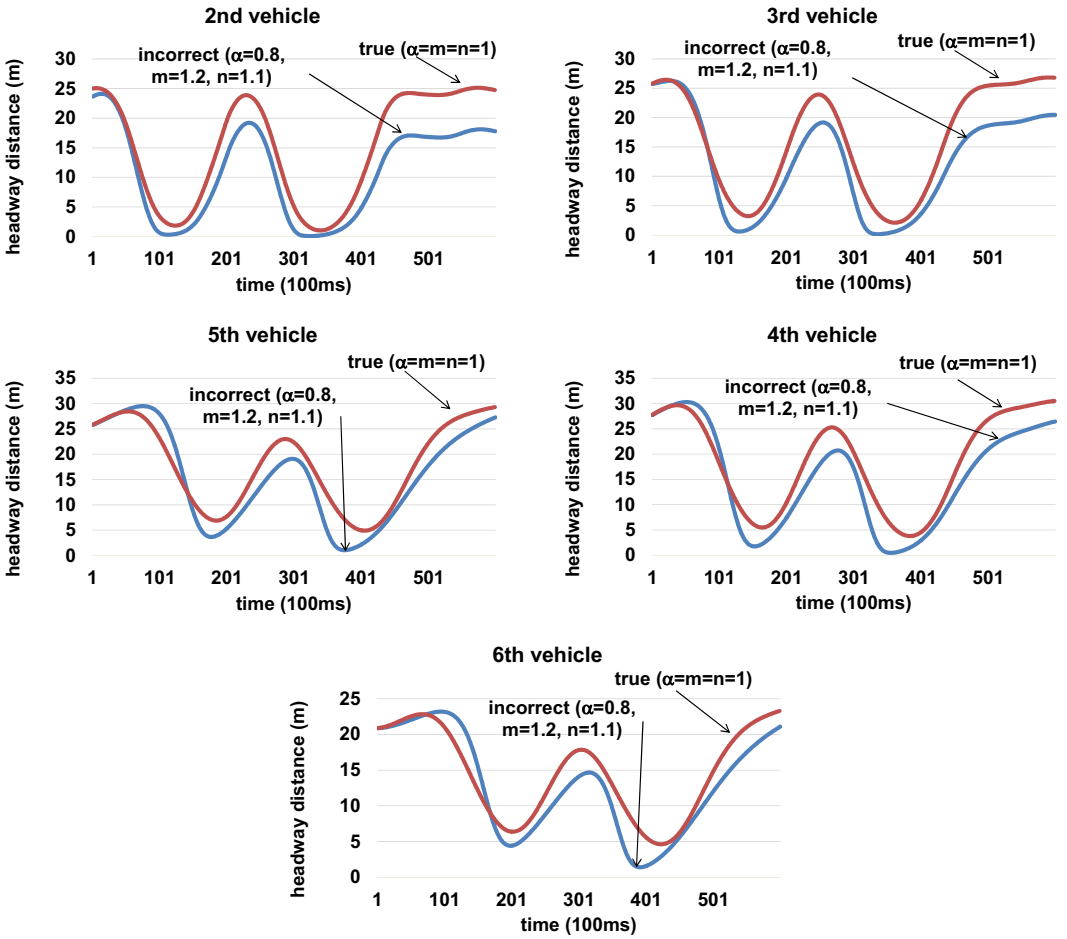

Fig. 3: Headway distances using different model parameter sets

4.3.2. Unexpected 3rd vehicle slowdown

In this portion of the study, it is assumed that the 3rd vehicle out of six in the platoon slows down unexpectedly during the car-following process. In such situations, as shown in Fig. 4, the headway distance of the 3rd vehicle becomes significantly longer than usual, and the following 4th to 6th vehicles travel with much shorter headway and at lower speeds. However, the GHR model itself is completely unable to describe the slowdown because no posterior information can be provided to the model in advance.

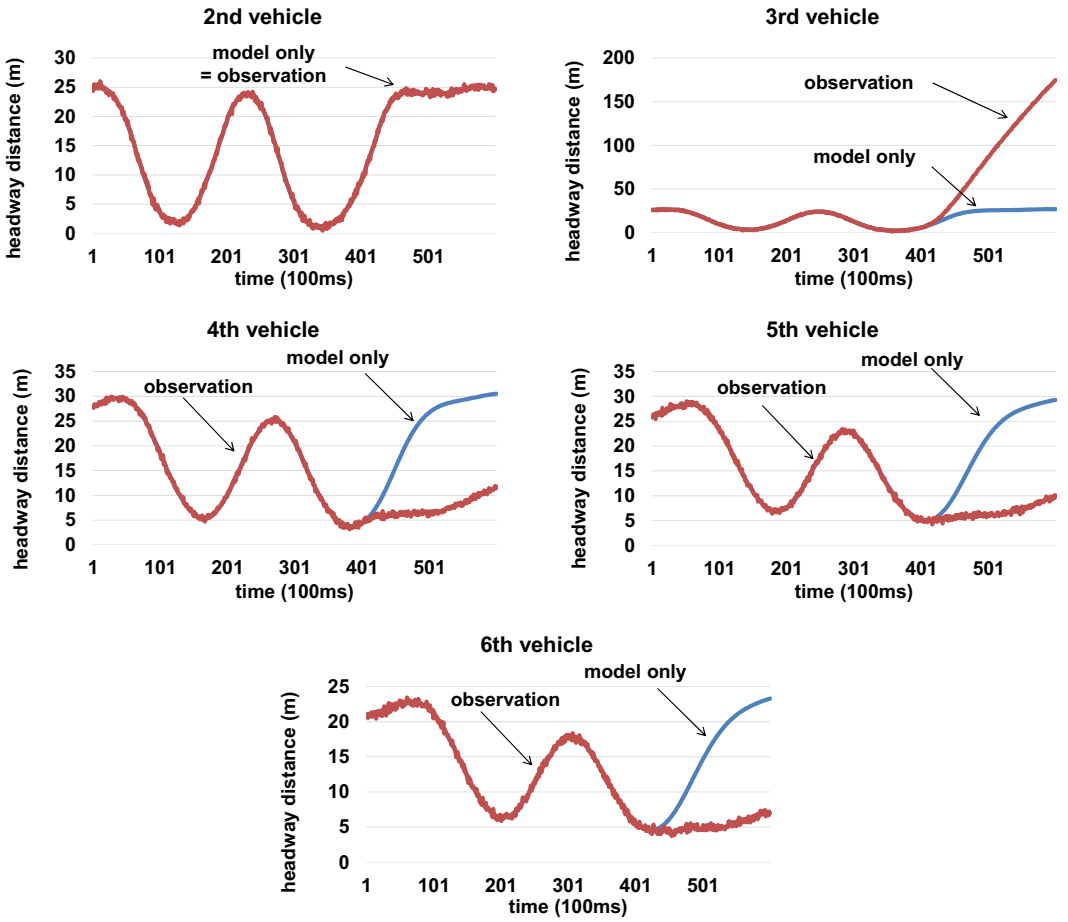

Fig. 4: Headway distance with and without unexpected 3rd vehicle deceleration

4.4. Four scenarios of numerical analysis

We artificially created four situations that would cause the simulated headway distance to deviate from the true observation. Our goal was to evaluate how much the PF and the UKF minimize the deviation by the feedback process under those scenarios, which are given in Table 1 below:

Table 1: Four Scenarios for Numerical Analysis

Assumptions / **Probe car installation**	**Wrong parameter of GHR car-following model**	**Unexpected slowdown of the 3rd vehicle**
Every two vehicles (2nd, 4th and 6th)	Scenario 1	Scenario 2
All vehicles (2nd to 6th)	Scenario 3	Scenario 4

In Scenario 2, it is especially notable that the slowdown of the 3rd vehicle could not be directly measured at the 3rd vehicle itself because the probe car sensors were only installed on the 2nd, 4th, and 6th vehicles. The PF and UKF were then used to detect the slowdown of the 3rd vehicle indirectly from the measurement of acceleration and velocity at the 2nd, 4th, and 6th probe cars.

4.5. Simulation parameter setting

The simulation time was set at 600 s and the time slice Δt was set at 0.1 s. The number of particles generated in the PF was 1000 for all scenarios. *ESSTH* was fixed at 15 based on the study by Nishida [Nishida, 2013]. In addition, the scaling factor λ in (16) was set to 1. The variance of system and measurement noises for the PF and the UKF executions are given in Table 2.

Table 2: Variance of System and Measurement Noises for the PF and the UKF Computations

Estimators	Variance of system noise (headway distance)	Variance of system noise (velocity)	Variance of measurement noise (acceleration rate)	Variance of measurement noise (velocity)
PF	0.2	0.2	0.1	0.2
UKF	0.4	0.4	0.1	0.2

4.6. Estimation results

4.6.1. Scenario 1 (observed at every two vehicles, wrong model parameter set)

Fig. 5 shows the headway distance estimation results of all five following vehicles. When compared to Fig. 3, it can be seen that the error caused by the incorrect model parameter set was significantly minimized through the PF and the UKF feedback. The PF estimates were close to the true headway, whereas some underestimations were found in the UKF feedback, especially at the probe cars (2nd, 4th, and 6th vehicles). This indicates that the PF is more capable of finding a true headway value, even when the car-following model parameters are incorrect. This is because the particles distributed around the nominal value cover the true mean and covariance appropriately. However, UKF accuracy depends strongly on the measurement equation described by the car-following model. Therefore, the model parameters should be as accurate as possible in order to increase the estimation accuracy when the UKF is applied. Furthermore, we determined that even though the UKF also performs well, it still faces limitations in terms of its ability to fully minimize errors caused by incorrect model parameters.

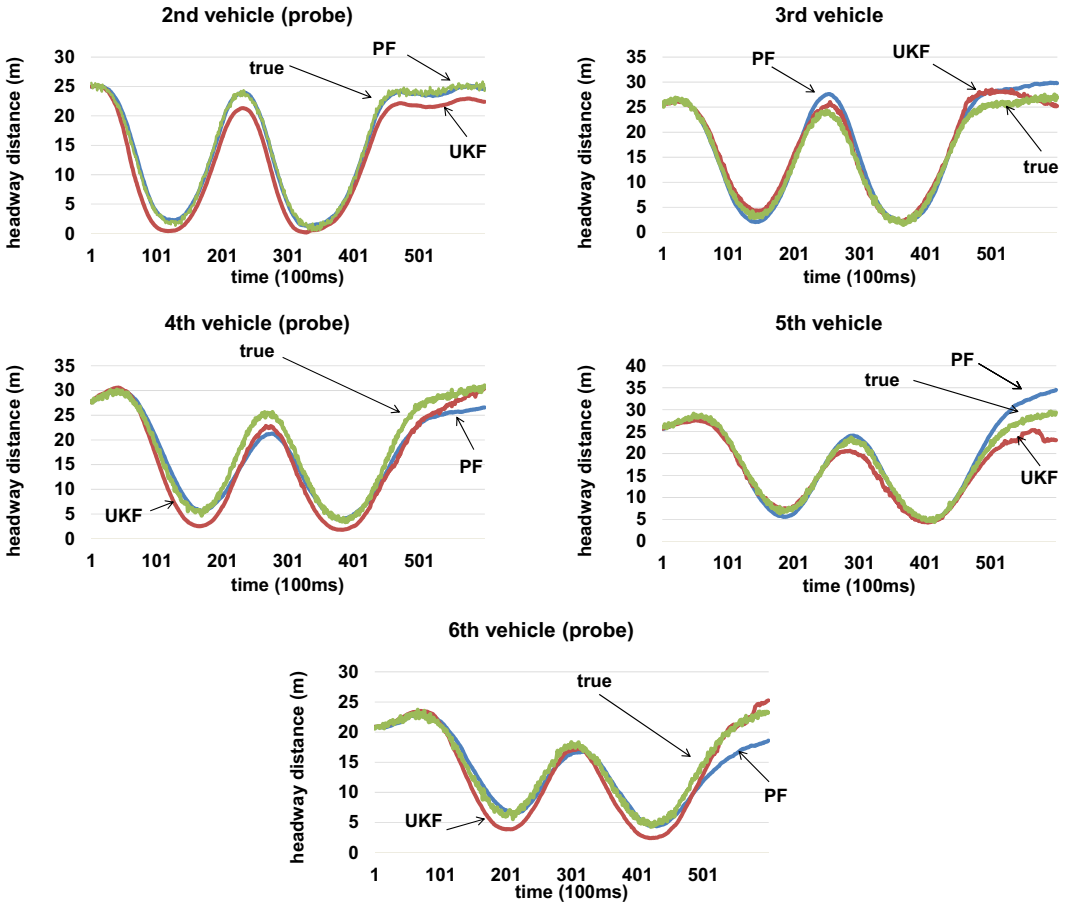

Fig. 5: Headway estimation by PF and UKF in Scenario 1 (observed at every two vehicles, incorrect model parameter set)

4.6.2. Scenario 2 (observed at every two vehicles, unexpected slowdown of the 3rd vehicle)

Precisely how the PF and the UKF estimated the unexpected 3rd vehicle slowdown is shown in Fig. 6. Again, it should be noted that the 3rd vehicle itself could not directly detect the slowdown. Instead, it was first identified at the 4th vehicle because the probe car sensors were only installed on the 2nd, 4th, and 6th vehicles. Both PF and UKF succeeded in detecting the 3rd vehicle slowdown without any direct measurement. However, it was clear that UKF performed much better and was more stable than PF, especially at the 3rd, 4th, and 6th vehicles. PF alone was unable to understand that the 4th and 6th vehicles follow the preceding vehicles just is if no slowdown had occurred in the 3rd vehicle. In an unexpected car-following situation that yields large errors between the model output and true headway, the PF particles should be more carefully generated and distributed to locations that are close to the target. In contrast, UKF was successful in estimating the true headway even when the slowdown was not directly measured at the slowdown vehicle itself.

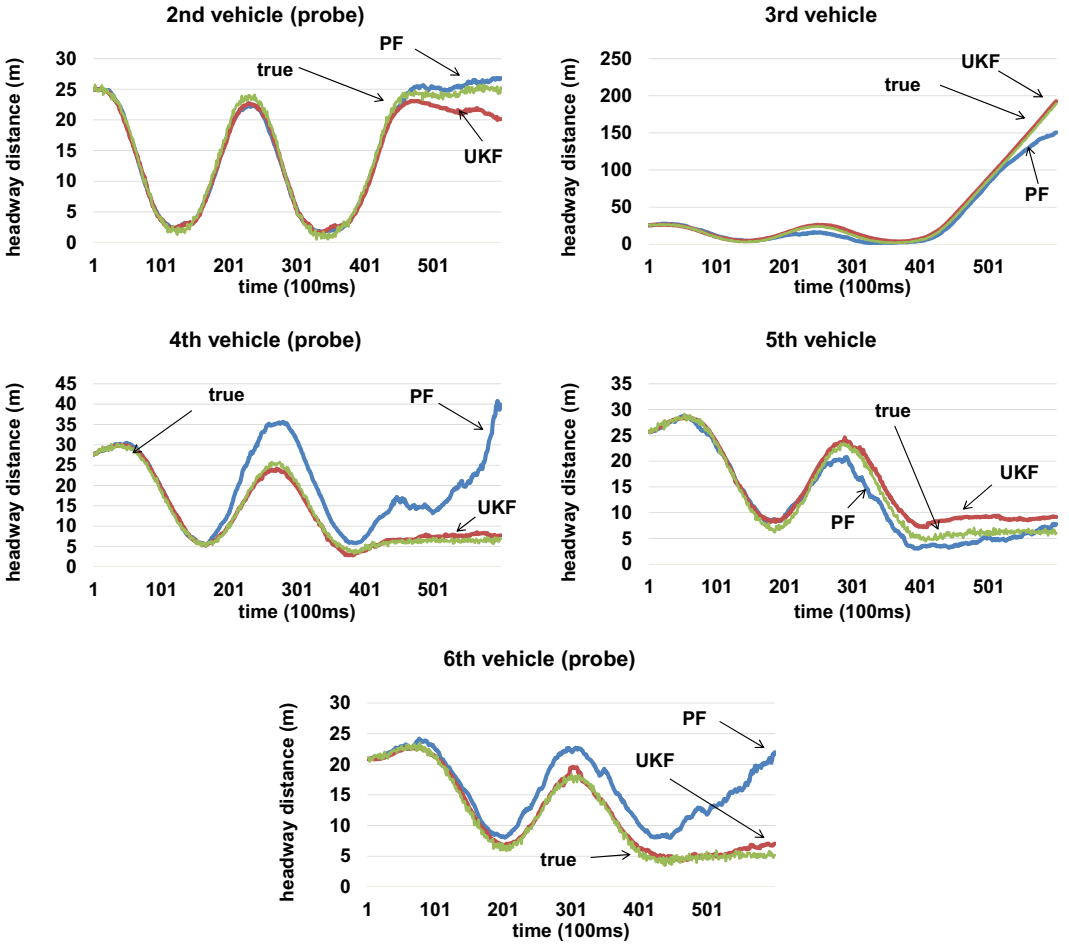

Fig. 6: Headway estimation by PF and UKF in Scenario 2 (observes at every two vehicles, unexpected 3rd vehicle slowdown)

4.6.3. Scenario 3 (observed at all vehicles, wrong model parameter set)

Fig. 6 depicts the headway estimation when the acceleration rate and velocity was measured at all five following vehicles. When compared to Scenario 1, in which only three vehicles were equipped as probe cars, the PF estimation accuracy was found to have increased and the estimates were very close to the true headway. However, when the UKF was applied, the underestimation was more significant than recorded in Scenario 1 because the UKF is significantly affected by the accuracy of the car-following model, especially at the observation vehicle. Therefore, it was determined that the UKF needs the car-following model to be as accurate as possible in order to output sufficient estimation precision, even though the PF proved to be very robust against the model parameter deviation.

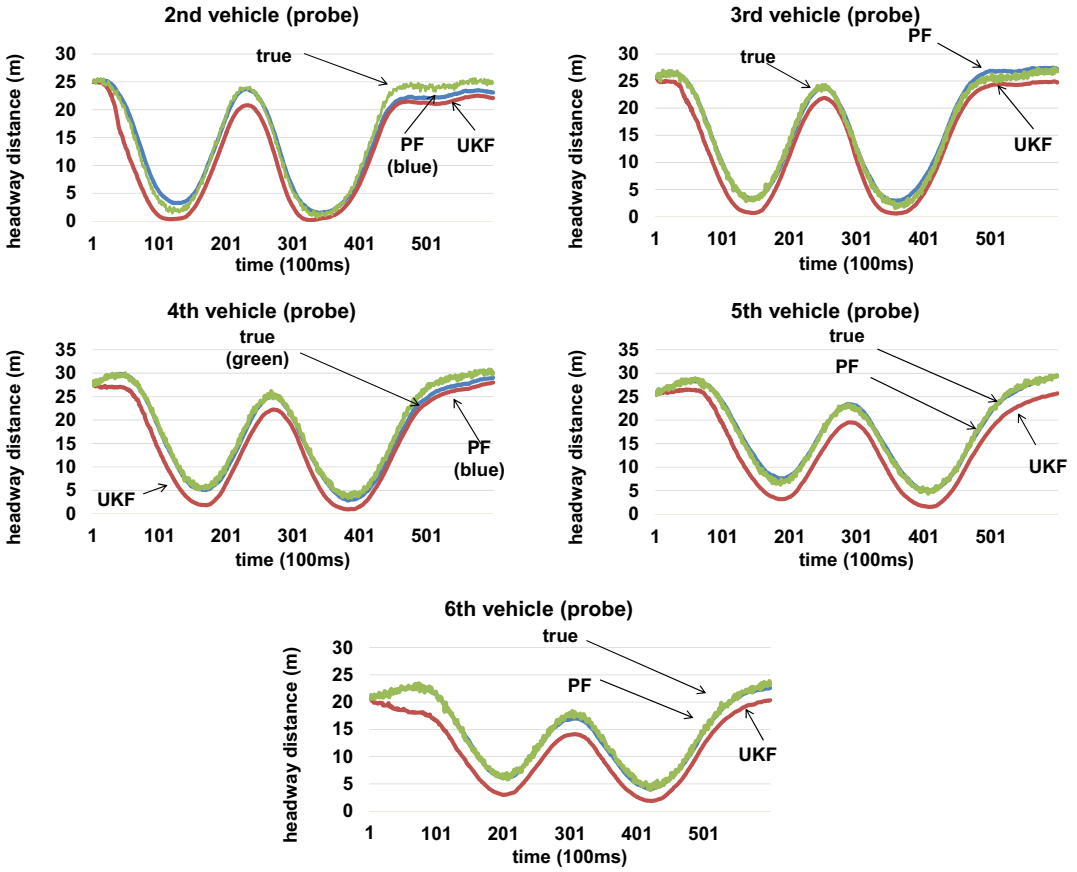

Fig. 7: Headway estimation by PF and UKF in Scenario 3 (observed at all vehicles, wrong model parameter set)

4.6.4. Scenario 4 (observed at all vehicles, unexpected slowdown of the 3rd vehicle)

When sensors are installed in all vehicles, the unexpected slowdown of the 3rd vehicle could be precisely detected by the PF and the UKF in order to yield the more accurate headway distance. Compared to Scenario 2 in Fig. 5, in which the probe car sensors were only installed in every two vehicles, both the PF and the UKF estimation accuracy improved significantly. If all vehicles were equipped as probe cars, and thus capable of determining the acceleration rate and velocity, the PF performs better than the UKF in any situation where the model output and true headway deviate.

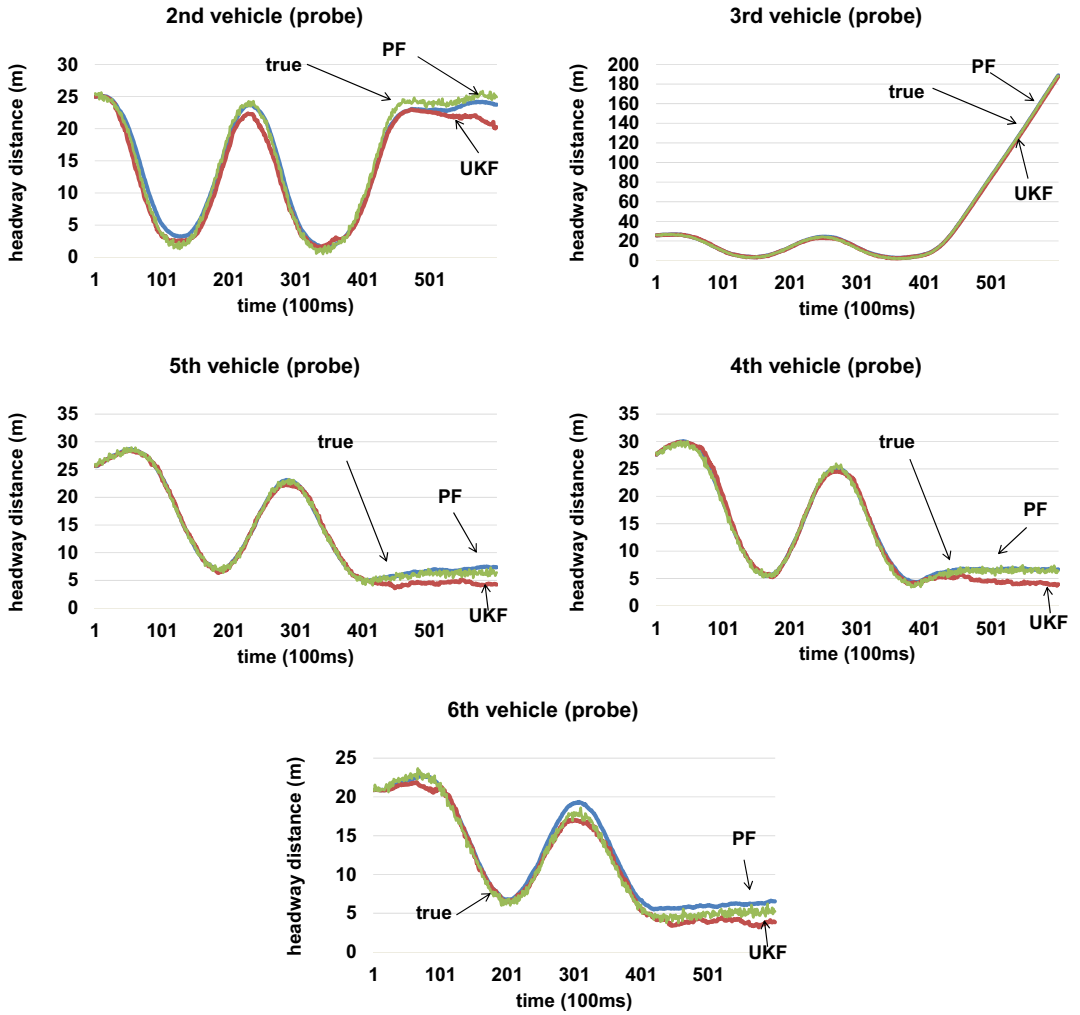

Fig. 8: Headway estimation by the PF and the UKF in Scenario 4 (observed at all vehicles, unexpected slowdown of the 3rd vehicle)

4.7. Discussion

As demonstrated above in the numerical example, both the PF and the UKF were found to be capable of estimating the headway distance, even in situations where the car-following model does not express the true car-following phenomena. However, it is also true that both the PF and the UKF have advantages and disadvantages, which can be summarized as follows:

- The PF is very robust when encountering model parameter deviation, but is unable to describe unexpected car-following situations unless the acceleration rate and velocity are measured at all probe vehicles. However, regardless of the number of probe cars, the errors caused by the wrong model parameters were significantly reduced.
- The UKF cannot fully minimize the errors caused by an incorrect model parameter set because its accuracy strongly depends on how precisely the measurement equation describes the car-following process. Therefore, improvements can be expected if the model parameter set itself is also corrected to the true values. However, it is significant that the UKF is capable of detecting the unexpected slowdown of a vehicle more precisely than PF, even if the number of probe cars in the platoon is insufficient.

These findings were also confirmed by examining the root mean square errors (RMSE) of the headway estimation, as shown in Fig. 9. As shown, if all the vehicles are equipped as probe cars capable of measuring acceleration rate and velocity, the PF is superior to the UKF in its ability to estimate the headway distance more precisely in all cases where the model output and true headway deviate. Furthermore, if measurements are not taken at all vehicles, the UKF is as stable as or more than the PF, especially when a vehicle in the platoon unexpectedly slows down during the car-following process. To increase estimation accuracy, it will be necessary to ensure that the headway distance and the car-following model parameters can be estimated simultaneously within a single estimation process.

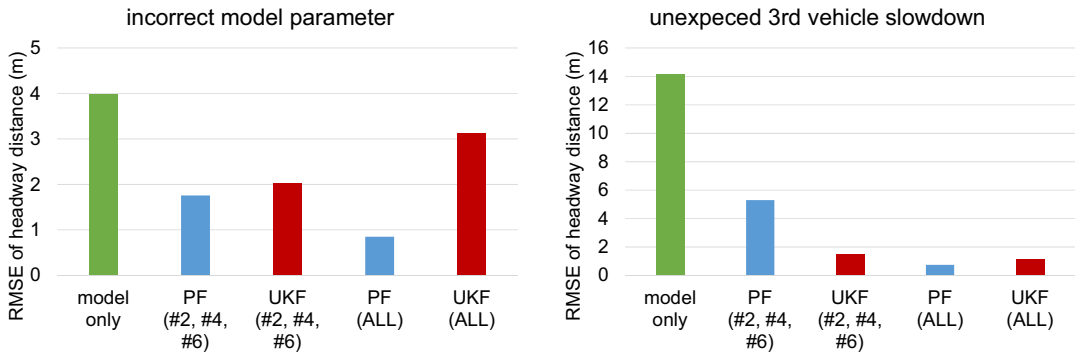

Fig. 9: Mean RMSE of headway distance

5. Conclusion

In this study, we applied a PF and a UKF to estimate the headway distance of platooned vehicles in a case where the prior knowledge of the model parameters was different from actually observed posterior information. Another scenario was prepared to evaluate the performance of the PF and the UKF in a situation where a vehicle in a platoon slowed down unexpectedly during the car-following process. In other words, the PF and the UKF were employed to minimize the errors in headway distance caused by the incorrect model parameters and unexpected vehicle slowdown.

Assuming a six-vehicle platoon, the headway distances of the following five vehicles were indirectly estimated by measuring the acceleration rate and velocity of three vehicles, or of all vehicles, in the platoon. It should be noted that direct measurements using costly laser or radar sensors were not required in this estimation system.

Numerical analysis showed that both the PF and the UKF successfully estimated the headway distance, even when in situations where the car-following model did not always express the car-following phenomena precisely. However, it was also found that both the PF and the UKF have unique advantages and disadvantages. For example, PF is very robust in terms of dealing with model parameter deviations, but was generally unable to accurately describe unexpected car-following situations unless the acceleration rate and velocity could be measured at all probe vehicles. On the other hand, we found that UKF accuracy was strongly affected by how precisely the model describes the car-following process, which meant that it was unable to minimize the errors caused by the incorrect model parameters. In spite of this disadvantage, it should be noted that the UKF was capable of detecting the unexpected slowdown of a vehicle more precisely than PF, even if a reduced number of probe cars were included in the platoon.

Therefore, it can be concluded that if all vehicles in a platoon are equipped as probe cars capable of measuring the acceleration rate and velocity, the PF is superior to the UKF and can estimate the headway distance more precisely. In contrast, if measurements are not conducted at all vehicles, the UKF is more stable than the PF, especially when a vehicle in the platoon unexpectedly slows down during the car-following process. To increase estimation accuracy, especially in situations when the parameter set of the car-following model is incorrect, it will be necessary to ensure that the headway distance and the parameter set itself can be estimated simultaneously by the PF and/or the UKF within a single estimation process. This “dual” estimation process is referred to as the dual PF, or a dual UKF, and it has already been confirmed that the dual estimation process improves estimation accuracy

[Wan and Nelson (2001)]. Further studies should be aimed at modeling the dual PF or dual UKF that will be applied to the dual estimation of headway distances and car-following model parameters.

Acknowledgements

This work is supported by JSPS KAKENHI Grant Number C24510231.

References

Arulampalam, M.S., Maskell, S., Gordon, N., Clapp, T., 2002. A tutorial on particle filters for online nonlinear/non-Gaussian Bayesian tracking, IEEE Transcactions on Signal Processing, Vol. 50, No. 2, 174-188.

Blake, A., Isard, M. & MacCormic, J., 2001. Statistical Models of Visual Shape And Motion, in "*Sequential Monte Carlo Methods in Practice*". In: Doucet, A., de Freitas, N., Gordon, N.(Ed.). Springer, 339-358, 2001.

Doucet, A. & Johansen, A.M., 2011. A Tutorial On Particle Filtering And Smoothing: Fifteen Years Later, Oxford Handbook of Nonlinear Filtering.

Fox, D., Thrun, S., Burgard, W., & Dellaert, F., 2001. Particle Filters For Mobile Robot Localization, in "*Sequential Monte Carlo Methods in Practice*". In: Doucet, A., de Freitas, N., Gordon, N.(Ed.). Springer, 401-428.

Ikoma, N., 2012. Sequential Monte Carlo Method And Particle Filter, Chapter 11, Vol. III, In: Statistical Science of 21 Century. HP edition; Japan Statistical Society. (in Japanese)

Marumo, Y., Tanaka, K., & Suzuki, H., 2013. Assistance System To Predict Driving Behavior Considering Information On Pre-Preceding Vehicle", *Second International Symposium on Future Active Safety Technology* (FAST Zero).

McGinnity, S. & Irwin, G.W., 2001. Maneuvering Target Tracking Using A Multiple-Model Bootstrap Filter, in "*Sequential Monte Carlo Methods in Practice*". In: Doucet, A., de Freitas, N., Gordon, N.(Ed.). Springer, 479-498.

Nishida, T., 2013. State Feedback Control Using Particle Filter, *IEEJ Trans. on Electronics, Information and Systems*, Vol.133, No.7, 1376-1283. (in Japanese)

Pueboobpaphan, R., Nakatsuji, T., & Suzuki, H., 2007. Unscented Kalman Filter-Based Real-Time Traffic State Estimation, presented at *Transportation Research Board 86th Annual Meeting,* TRB 86th Annual Meeting Compendium of Papers CD-ROM.

Pueboobpaphan, R., & Nakatsuji, T., 2011. Assignment-Matrix-Free Dynamic Estimation Of Origin-Destination Matrices, *Journal of Japan Society of Civil Engineers, Ser. D3 (Infrastructure Planning and Management)*, Vol. 68, No. 3, 327-338.

Rothery, R.W., 1998. Car following models, in "*Revised Monograph On Traffic Flow Theory*". In: Gartner, N. Messer, C. J., Rathi, A. K. (Ed.). FHWA.

Suzuki, H. & Nakatsuji, T., 2013. Feedback Estimators For Identifying Headway Distance And Velocity Of Longitudinal Platooned Vehicles, *Journal of the Eastern Asia Society for Transportation Studies*, vol. 10, 1631-1649, published at http://dx.doi.org/10.11175/easts.10.1631.

Suzuki, H., 2013. Dynamic State Estimation In Vehicle Platoon System By Applying Particle Filter And Unscented Kalman Filter, *Procedia Computer Science*, Vol. 24, 30-41, 17th Asia Pacific Symposium on Intelligent and Evolutionary Systems, IES2013, published at http://dx.doi.org/10.1016/j.procs.2013.10.025.

Takada, S., Hiraoka, T. & Kawakami, H., 2012. Effect of Forward Obstacles Collision Warning System Based On Deceleration For Collision Avoidance On Driving Behavior, *Proceedings of 19th World Congress on Intelligent Transport Systems*.

Wan, E. A., Nelson, A. T., 2001. Dual Extended Kalman Filter Method, in "*Kalman Filtering and Neural Networks*". In: Haykin, S. (Ed.). John Wiley & Sons, 123-173.